#7648 LIDAR-BASED SOYBEAN CROP SEGMENTATION FOR AUTONOMOUS NAVIGATION

V.A.H. Higuti, A.E.B. Velasquez, M.V. Gasparino, D.V. Magalhães, R.V. Aroca, D.M.B.P. Milori, M. Becker
University of São Paulo, São Paulo, Brazil
becker@sc.usp.br +55 16 3373 8646

ABSTRACT

This study describes how a 2D LiDAR (Light Detection and Ranging) can be combined with ground mobile robot's odometry to generate a 3D point cloud to represent the surroundings, e.g. a soybean crop. Additionally, it also shows how the robot interprets the point cloud to allow autonomous row following without the most common positioning source: GNSS (Global Navigation Satellite System). Experiments were carried out with a 4WSD (four-wheel steering and drive) robot in a soybean research crop to verify the behavior of the proposed system.

INTRODUCTION

The technological advances in the last few decades have greatly changed agriculture. Modern farms have adopted sophisticated technologies, such as sensors, aerial images, and GNSS (Global Navigation Satellite System) to become safer, more profitable, efficient, and sustainable. These technologies not only increase the crop productivity, but also reduce the wide use of water, fertilizers, and pesticides. Due to this, they reduce costs and negative environmental impacts, such as the contamination of water sources. In special, the use of mobile robots has allowed more reliable monitoring and management of natural resources (NIFA, n.d.).

However, the application of robotics in agriculture is still challenging and researchers are seeking smarter autonomous vehicles that can safely operate in semi-structured or unstructured dynamic environments, where humans, animals, and agricultural machinery may be present. The most common sensor types used are cameras, LiDAR (Light Detection and Ranging), GNSS, inertial sensors, and encoders. Real Time Kinematics GNSS has allowed the autonomous operation of many machinery due to its highly accurate positional information when a clean view of satellites is possible. Nevertheless, such systems cannot handle dynamic obstacles, and their performance may degrade due to uncontrollable sources that affect the satellites signals. To guarantee safety in scenarios where GNSS may fail, cameras and/or LiDAR can be used (Reina et al., 2016).

Although vision systems are commonly used in mobile robot navigation, they suffer from high variation of lighting conditions in outdoor environments and the large amount of data from camera is still a severe compromise between robustness and available processing power in mobile robots. Other sensors (e.g. LiDAR, ultrasound, and infrared) are used to measure absolute distances. Among them, LiDAR have greatly benefited from cost reductions while maintaining a fast, high range, and millimeter-level measurement (Bechar & Vigneault, 2016). Some works, including others in our laboratory, use a 2D LiDAR parallel to ground. This assumes that rows are taller than the sensor and that horizontal reading planes provide similar information. However, soybean grows in branches and main stem may not always be visible. This confers a bushy shape that may be misleading if sensed only in a single horizontal plane. Moreover, the sensor would need to be positioned too close to ground to read plants at

earlier stages, which is either dangerous for device safety or it requires additional structural solutions.

In this paper, we describe the deployment of a perception system based on two 2D LiDAR sensors for the navigation of an agricultural robot in soybean crops. The proposed system takes advantage of the robot's movement, which is tracked by odometry, to create a 3D point cloud by concatenating consecutive 2D LiDAR readings. This setup can be referred as a push-broom (Baldwin and Newman, 2012) and it has the cost advantage when compared to an off-the-shelf 3D LiDAR and dismisses additional hardware to obtain more degrees of freedom to the sensor, e.g. rotation/translation around one axis to have multiple reading planes over time.

MATERIALS AND METHODS

This study follows a similar process as presented by Gasparino et al., 2020: a laser reconstruction, data filtering, and determination of navigable space. In the first step, we change from an active method to create the multilayered point cloud (custom hardware to rotate the sensor) to a passive one (push broom). In data filtering, the Gaussian multiplication step is replaced by a threshold. Finally, the determination of navigable space changes from Under Canopy LiDAR-based Perception Subsystem (Higuti et al., 2018) to a histogram.

The locomotion system is composed of four modules linked by a passive suspension. Each one has a motor for traction and another for steering. All motors are electric, and they are controlled by ESCON 50/5 (traction) or EPOS 24/5 (steering). An industrial computer Advantech ARK-3510 running Ubuntu 16.04 with Robotic Operating System (ROS) Kinetic performs all computational tasks. Further information may be found in Higuti et al., 2017.

Two types of sensor provide the information to perform the environment recognition. First, UTM30-LX Hokuyo is a 2D LiDAR that returns 1081 distance readings over a 270º range with 40 Hz update rate. One LiDAR was placed on each frontal locomotion module, hence one to the left and another to the right, in a way that wheels and the sensor are aligned on the same longitudinal line and at a height of around 0.65 m from ground (see red circles in Fig. 1a). They point downwards such that sensors' field of view forms an angle of 60º with ground plane. Second, MILE encoders provide the traction motors' rotational speed and steering motors' position.

The proposed system starts with the generation of a 3D point cloud from sensor data. A single 2D laser scan provides distance measurements only on the sensor's reading plane (see orange features in Fig. 1b). Therefore, when the robot moves, the scans are assembled considering the robot movement, creating a local 3D crop reconstruction. In this study, the targeted forward speed is small (maximum of 0.3 m/s) and the terrain is regular, without bumps and/or weed infestation. Furthermore, Mirã 2 passive suspension keeps all wheels with contact to ground. These reasons allow us to conclude that slippage and dynamic interaction between wheels and soil have negligible interference to estimate the instantaneous robot's position with an odometry based on robot kinematics (Jazar, 2014; Rajamani, 2006; Khristamto et al., 2015).

The odometry estimates the center of mass position, a point that represents the robot, which was determined using the method presented in Velasquez, 2015 and Jazzar, 2014. The position of center of mass is given on a cartesian reference frame (XY coordinates) whose origin is set as the position where the robot starts moving autonomously, usually the begin of the lane. Angular and linear velocities are integrated over time to estimate the current position of center of mass. The velocities are calculated using Ackermann geometry (Jazar, 2014), a set of kinematic equations that relates the wheels direction and speed into robot's linear and angular velocities. The steering

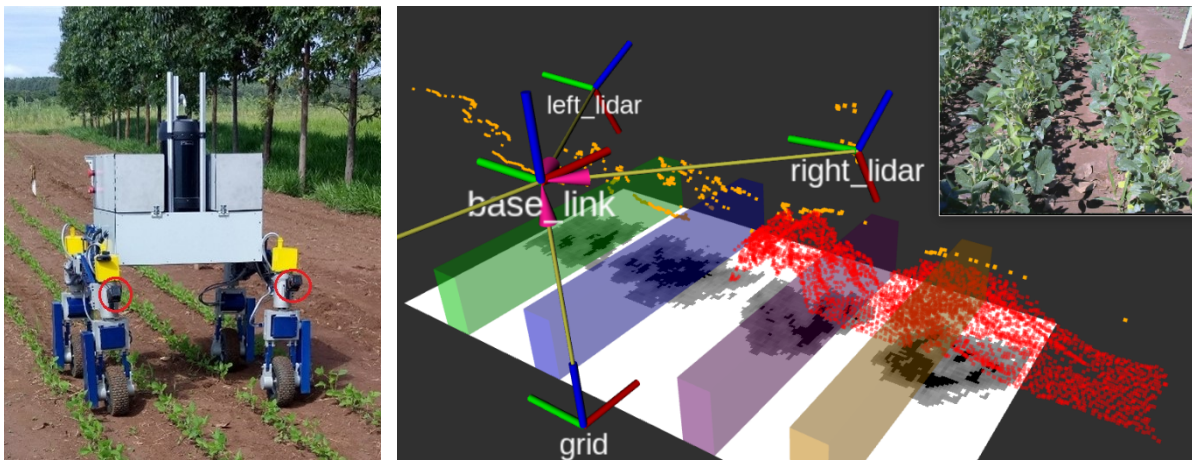

(a) (b)

Figure 1. (a) Mirã 2 in the soybean crop; (b) The axes show some reference frames: base_link is placed on the robot's center of mass; right_lidar and left_lidar represent how LiDAR sensors are placed with respect to center of mass – note that the reading plane is given by red and green axes, therefore an angled plane towards ground; and grid's red and green axes represent the ground plane. The last LiDAR scan from the left sensor is shown by orange points, the red set is the resulting point cloud for right side, the grids are the white rectangles with gray/black elements, and the navigable space is bounded by the green/blue or purple/brown boxes.

motor encoders inform the wheel direction and those from traction motors provide the wheel speed.

After center of mass position is known, a static spatial transformation from center of mass to each LiDAR sensor allows us to know where each laser scan happened and two-point clouds (one from right and another for the left LiDAR sensor) are obtained by concatenating the scans (see the red point cloud in Fig. 1b). Each point cloud keeps 100 scans before throwing the old ones and it is downsampled using a voxel, i.e. a box, of 0.02 m size in all axes. This leaves enough detail while reducing subsequent processing time. These operations use Point Cloud Library.

Subsequently, the 3D point cloud is converted to a 2D occupancy grid, a discrete representation of navigable space on the plane parallel to ground. In this study, the grids have 100 rows, 90 columns and 0.02 m resolution. Their center point (between rows 49-50 and cols 44-45 with initial index 0) projects from the reading origin of LiDAR sensors down to the ground. This effectively removes the point cloud z-dimension as each grid cell contains the number of points from the point cloud that are within the cell XY-boundaries.

After grid is obtained, a mask enhances the cells that are in the column direction as they are mostly linked to the crop rows (most populated region in the point cloud). After this operation, the grid is normalized to have values between 0 and 100, with 100 given to the most populated cell. Subsequently, two thresholds are applied to the grid and those cells under 40% are set to 0 and those above 60% are set to 100, respectively white and black cells on the grid rectangle in Fig. 1b. The gray cells are in-between values. Finally, a histogram on row axis highlights two densest rows, one to the right and another to the left of sensor. These rows reflect the boundaries of the navigable space (represented by the long-colored boxes in Fig. 1b). Going back from grid units to XY coordinates, the distance to lateral rows (d_r for right and d_l for left) become known. For a control system designed to follow row, a cross track error can be calculated for each LiDAR as $cte = 0.5(d_r - d_l)$ and such value shows the error from the desired position, i.e. middle of row. In this study, the sum of lateral distances (lane width) will be used to assess the system performance because it can be compared to a nominal value and

variations along run and between runs on the same rows show how stable is the determination of navigable space.

RESULTS AND DISCUSSION

Field experiments were conducted at the National Reference Laboratory in Precision Agriculture (Lanapre) located in São Carlos, SP. Two plots with four soybean (Intacta RR2 Pro) rows each were planted. Distance between rows is 0.45 m within plot, total length is 32 m and plant spacing is about 12 plants/m. Tests happened 55 days after seeding.

A first set of tests evaluated a system like the one shown by Gasparino et al., 2020. Due to platform difference, it already differed in the laser reconstruction, which was done as explained in the previous section. It still used a multiplication of the grid by a sum of two Gaussian functions to highlight the most probable row position. Although that had effect for their study with corn, this failed to keep a constant boost to only the densest part of the row: different regions were enhanced in consecutive scans because of multiple branches. This led to navigable space changing more than a few centimeters between consecutive estimates. Such instability prejudiced control actions as the robot constantly thought it had a different navigable space than before. Additionally, the algorithm transformed from grid to a laser scan parallel to ground. This would enable the usage of the Under Canopy LiDAR-based Perception Subsystem (Higuti et al., 2018), which was assessed for corn, sorghum and dry soybean. But that method was designed for crops with well-defined stems, even if sometimes occluded. This is not the case for early-mid soybean because of the high number of branches, and a similar behavior as from the Gaussian use happened: unstable definition of a lateral distance. With such system, the robot could barely move few meters without hitting.

After changes described in this study, the robot completed 22 of 28 runs (78% success rate). The six failures occurred due to mechanical restrictions or an oscillatory behavior caused by the control system. The following reported values reflect an average value for a run, if not specified. Left LiDAR calculations gave lane width in the range of 0.323-0.406 m and standard deviation between 0.063-0.156 m. Analogously, right LiDAR had lane width in the range 0.363-0.423 m and standard deviation of 0.041-0.157 m. As these runs occurred on the same soybean rows, these variations show that perceived navigable space is still not continuous enough, which may have led the control to believe the robot had more/less room to operate than it truly had and made oscillating commands. Indeed, with respect to each run's average value for successful runs, left LiDAR had only 37-61% and right LiDAR had 42-62% of the instantaneous lane width within 0.05 m error (a comparable range expected from RTK GNSS). However, this increases to 75-83% (left) and 77-92% (right) for a 0.1 m error. Coupled with the 78% success rate to traverse the 32 m plot, this 0.1 m error seems reasonable to allow autonomous navigation. Hence, we concluded that the proposed perception system is a promising tool to detect the position of soybean crop rows.

ACKNOWLEDGEMENTS

Supported by Embrapa Instrumentation, University of São Paulo, Brazilian National Council for Scientific and Technological Development (CNPq), Coordination for the Improvement of Higher Education Personnel (CAPES) and São Paulo Research Foundation (FAPESP) with grants #2018/10894-2 and #2013/07276-1. The opinions, hypotheses, conclusions or recommendations expressed herein do not necessarily reflect those of FAPESP.

REFERENCES

Baldwin I, Newman P. 2012. Road vehicle localization with 2D push-broom LIDAR and 3D priors," *2012 IEEE International Conference on Robotics and Automation* 2611-2617.

Bechar A, Vigneault C. 2016. Agricultural robots for field operations: Concepts and components. Biosystems Engineering 149: 94–111.

Gasparino M, Higuti V, Velasquez A, Becker M. 2020. Improved localization in a corn crop row using a rotated laser rangefinder for three-dimensional data acquisition. Journal of the Brazilian Society of Mechanical Sciences and Engineering 45: 592.

Higuti V, Velasquez A, Gasparino M, Oliveira G, Carrasco C, Risardi J, Magalhães D, Becker M, Milori D. 2017. Robotic Platform with Passive Suspension to Be Applied on Soybean Crops: Initial Results. Proceedings of the 24th ABCM International Congress of Mechanical Engineering.

Higuti V, Velasquez A, Magalhaes D, Becker M, Chowdhary G. 2019. Under canopy light detection and ranging-based autonomous navigation. Field Robotics J. 36: 547–567.

Jazzar R, 2014. Vehicle Dynamics – Theory and Application. Springer. 2nd edition. 579-580.

Khristamto M, Praptijanto A, Kaleg S, 2015. Measuring geometric and kinematic properties to design steering axis to angle turn of the electric golf car. Energy Procedia 68: 463–470.

National Institute of Food and Agriculture (NIFA), n.d. Agriculture Technology. Available on https://nifa.usda.gov/topic/agriculture-technology

Rajamani R. 2006. Vehicle dynamics and control. Springer.

Reina G, Milella A, Rouveure R, Nielsen M, Worst R, Blas MR. 2016. Ambient awareness for agricultural robotic vehicles. Biosystems Engineering 146: 114-132.

Velasquez A. 2015. ℏELVIS III – Desenvolvimento e caracterização da plataforma robótica. Master dissertation, University of São Paulo.